

## ***Interactive comment on “Geomagnetic Conjugate Observations of Ionospheric Disturbances in response to North Korea Underground Nuclear Explosion on 3 September 2017” by Yi Liu et al.***

**Yi Liu et al.**

chenzhou@whu.edu.cn

Received and published: 28 December 2018

Review of the manuscript entitled “Geomagnetic Conjugate Observations of Ionospheric Disturbances in response to North Korea Underground Nuclear Explosion on 3 September 2017” by Liu et al., submitted for a possible publication in Annales Geophysicae [angeo-2018-122] General comment The manuscript describes observation of ionospheric disturbances induced by underground nuclear explosion (UNE) in North Korea on 3 September 2017. The ionospheric disturbances were observed both on the northern hemisphere and on southern hemisphere around conjugate point. The manuscript is reasonable well written, the subject is suitable for publication in Annales

C1

Geophysicae. I think that several points could be addressed more carefully to improve quality of the paper (see the specific comments). I recommend a moderate revision. Specific comments a) Section 2, the method of data analysis should be described in more detail. Specifically, the third-order horizontal 3-point derivative should be defined. It should be mentioned why such a derivative was used, and discussed its advantage with respect to standard first derivative. The authors reference to paper by Park et al. (2011) in this respect, however, I have not found a sufficient definition and discussion related to this derivative in their paper. Also, the procedure of removing background noise by using wavelet decomposition should be briefly described.

Response: We appreciate the reviewer for the valuable comment. The IGS stations used in this study are located in East Asia and Australia. The geographical positions of the UNE and the IGS stations are showed in Figure 1. In order to eliminate the noise and multipath effects of GPS signals, only carrier phase observations are utilized to derive the relative slant total electron content (STEC). The time resolution is about 30 s. The ionospheric pierce points (IPPs) height in this study is assumed at 350 km. Figure 2 shows an example of time series of relative STEC obtained by SUWN using satellite PRN 28 between 03:00-05:00 UT on 3 September 2017. To calculate the ionospheric disturbances related to UNE from GNSS observations, the main trends of relative STEC strongly influenced by the Sun's diurnal cycle need to be removed. In this study, the numerical third-order horizontal 3-point derivatives of relative STEC are used for extracting the ionospheric disturbances (Park et al., 2011). In the first step, the numerical first-order horizontal 3-point derivatives are taken as follows: (1) where is the  $i$ th data point, is the first derivative, and  $n$  is the number of relative STEC observations. The main relative STEC trends are removed through this process. Figure 3(a) shows the time series of first-order derivatives of relative STEC. Waves with small amplitudes occurred at around 3.9 and 4.1 hours, even though it was not certain whether they were meaningful signals or just noises. The numerical derivative formula is repeatedly performed on relative STEC derivatives to extract the ionospheric disturbances related to UNE. The second-order derivatives can be written in the following expression: (2)

C2

where is the second derivative, and  $m$  is the number of first derivative observations. Figure 3(b) shows the time series of second-order derivatives of relative STEC. Compared to the first-order derivatives presented in Figure 3(a), the amplitude around the 3.9 hour was amplified while others were not significant. The third-order derivatives are given as follows: (3) where is the third derivative, and  $l$  is the number of second derivative observations. Figure 3(c) shows the time series of third-order derivatives of relative STEC. Compared to the second-order derivatives presented in Figure 3(b), the disturbances around the 3.9 hour was further amplified. Therefore, compared to the standard first derivatives, the numerical third-order horizontal –point derivatives can emphasized the more significant wave components with small amplitudes. Moreover, to further remove the background noises of third-order derivatives of relative STEC, the harr wavelet decomposition process is applied to the third-order derivatives. Equations (4) and (5) give the harr wavelet function and scale function, respectively. (4) (5) Figure 3(d) shows the wavelet de-noised third-order derivatives. From Figure 3(d), it was found that the background noises in Figure 3(c) were completely removed and only valuable wave components were retained.

b)line 113-114 and Figure 3, I suggest comparison with average values calculated for 15 quite days before and after the UNE event rather than for only one day before the event. Also, I would recommend locating the modified text related to current Figure 3 after the text related to current Figure 5 (after line 125), and renumbering Figure 3 to Figure 6 (renumber Figure 4 to Figure 3). Current Figures 2 and 4 and the corresponding texts are closely related. I thing that the flow of information will be more logical in the suggested re-organization. In addition, insert explanation of black and green triangles in the text related to Figure 5 (current lines 123-125).

Response: We appreciate the reviewer for the valuable comment. We present the quiet time FAC derivatives and IRC derivatives for 15 quiet days before and after the UNE event in Figure 6. It was found that ionospheric current derivatives remained smooth in quiet time. By comparing with quiet time observations, obvious short-period fluctua-

C3

tions of ionospheric current derivatives at conjugate hemispheres were observed after the UNE in Figure 6(c) and Figure 6(d).

Figure 7 shows the horizontal distance from IPPs to epicenter and time delay of the UNE-generated ionospheric disturbances (STEC disturbances and ionospheric current disturbances). Therefore, we have renumbered Figure 5 to Figure 6 (renumber Figure 6 to Figure 5). Black triangle and green triangle presented in Figure 7 represent the position of ionospheric current disturbances in the northern hemisphere and the geomagnetic conjugate position of ionospheric current disturbances in the southern hemisphere, respectively.

c) Discussion, paragraph related to similarity with earthquakes. It should be mentioned, e.g., after the sentence Klimenko et al (2011) . . .that there were several studies that showed that co-seismic ionospheric disturbances were caused by long-period infrasound waves that propagated nearly vertically to ionospheric heights (Chum et al., 2016; Liu et al., 2016, Chum et al., 2018 and references therein). Chum, J., J.-Y. Liu, K. Podolská, T. Šindelářová (2018), Infrasound in the ionosphere from earthquakes and typhoons, *J. Atmos. Sol. Terr. Phys.*, 171, 72-82, doi:/10.1016/j.jastp.2017.07.022 Chum, J., M. A. Cabrera, Z. Mošna, M. Fagre, J. Baše, and J. Fišer (2016), Nonlinear acoustic waves in the viscous thermosphere and ionosphere above earthquake, *J. Geophys. Res. Space Physics*, 121, doi:10.1002/2016JA023450. Liu et al., (2016) is already in the references

Response: We appreciate the reviewer for the helpful suggestion. We have followed the reviewer's suggestion and added these references in the revised manuscript.

d) lines 180-181, LAIC electric field can be roughly estimated to be 11 mV/m. Specify the method of estimation.

Response: We appreciate the reviewer for the valuable comment. LAIC electric field can be roughly estimated by the following expression: (6) where is the total propagation velocity of ionospheric disturbances,  $E$  is LAIC electric field, and  $B$  is the magnetic field.

C4

Based on the LAIC electric field penetration model proposed by Zhou et al. (2017), it is found that LAIC electric field is perpendicular to the magnetic field. Therefore, total propagation velocity of ionospheric disturbances generated through  $E \times B$  drift can be calculated by . The value of horizontal velocity obtained by the least square estimation was  $\sim 280$  m/s in this study. Total magnetic field intensity and magnetic inclination angle  $I$  around UNE test site calculated by International Geomagnetic Reference Field (IGRF) model were  $4.39 \times 10^{-5}$  T and  $57.90^\circ$ , respectively. Therefore, LAIC electric field can be roughly estimated by equation (6) to be 14.5 mV/m.

e)Figure 5, related text and discussion. Specify, if the least square fitting was done under assumption that the fitted line goes through the beginning (point [0; 0]) or if an arbitrary offset along the vertical axis was admitted. If the arbitrary offset (preferred in my opinion) is admitted then from the obtained time delay at distance 0, one could say something about the time delay between explosion and ionospheric perturbation just above the explosion. Likely, one should have observation close to the explosion to obtain reliable results (time delay with sufficient precision). Anyway, theoretically, knowledge of this time delay could help to distinguish if the electric fields penetrated from below (from the ground) or if they were generated in the ionosphere. Note that there is a possibility that mechanic perturbations caused by AGWs change the electric conductivity in the lower ionosphere, which in turn, in the presence of (zonal) electric fields can cause horizontal perturbation of these background electric fields and associated currents that can be detected as geomagnetic perturbations (e.g. Liu et al., 2016). A possibility of such a mechanism should be briefly mentioned/discussed for completeness.

Response: We appreciate the reviewer for the valuable comment. We agree with reviewer's point that the knowledge of this time delay between explosion and ionospheric perturbation just above the explosion could help to distinguish if the electric fields penetrated from below (from the ground) or if they were generated in the ionosphere. However, in this work, we found that there is no relative STEC observations

C5

from IGS stations close to the UNE test site during the UNE events. Therefore, it is no way to investigate the time delay.

The physical mechanism that the electric field perturbations can be generated in the ionosphere has been briefly discussed in the revised manuscript. Please see Page 10 Line 186-192.

Technical comments (Minor or formal comments and language suggestions) -line 45, naturally processes-> natural processes -lines 46-47, coupled upper atmospheric variations – specify or remove -line 71, conductivity of the geomagnetic. .->conductivity along the geomagnetic -line 91, . . .temporal evolution which consists of. .->. . .temporal evolution. SWARM mission consists of. . -line 153, . . .indicated the abnormal. .->. . .indicated that the abnormal. . . Also, add a suitable reference after this sentence

Response: We appreciate the reviewer for the valuable comment. We have corrected accordingly. We would like to thank the reviewer again for the valuable comments, which help a lot to improve the quality of the present paper. We hope that the reviewers will be satisfied with our responses and revisions, and we look forward to hearing from the reviewers soon.

Reference: Park, J., Frese, R. R. B. von, Grejner-Brzezinska, D. A., Morton, Y., and Gaya-Pique, L. R.: Ionospheric detection of the 25 May 2009 North Korean underground nuclear test, *Geophys. Res. Lett.*, 38, L22802, 2011. Zhou, C., Liu, Y., Zhao, S., Liu, J., Zhang, X., Huang, J., Shen, X., Ni, B., and Zhao, Z.: An electric field penetration model for seismo-ionospheric research, *Adv. Space Res.*, 60(10), 2217-2232, 2017.

Please also note the supplement to this comment:

<https://www.ann-geophys-discuss.net/angeo-2018-122/angeo-2018-122-AC1-supplement.zip>

Interactive comment on *Ann. Geophys. Discuss.*, <https://doi.org/10.5194/angeo-2018-122>,

C6

C7

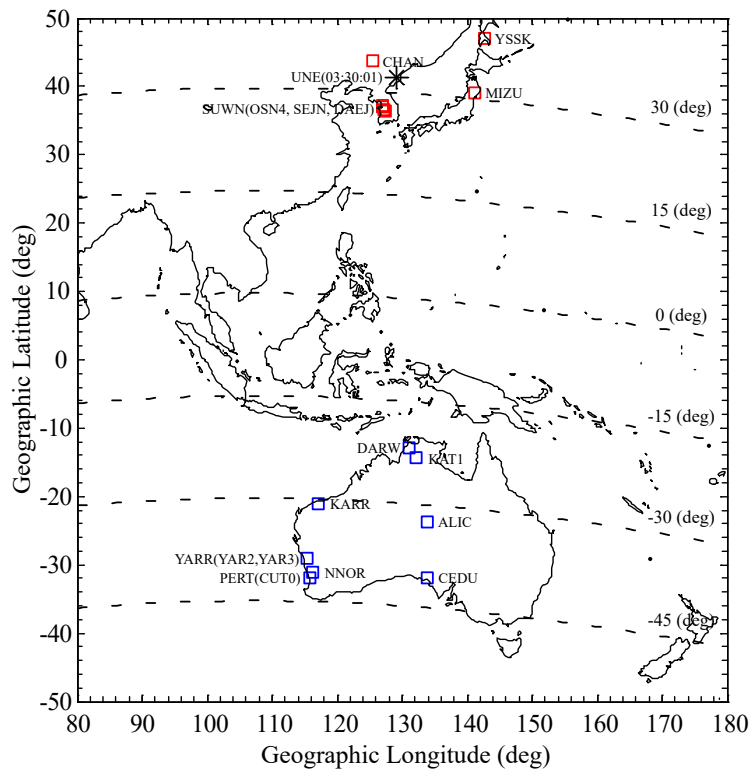


Fig. 1. Figure 1

C8

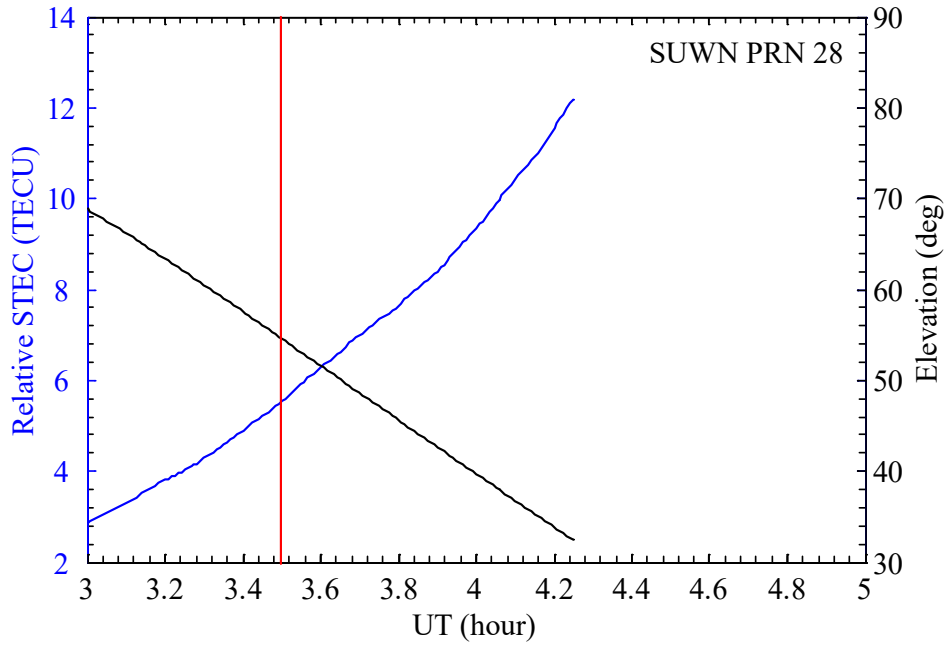


Fig. 2. Figure 2

C9

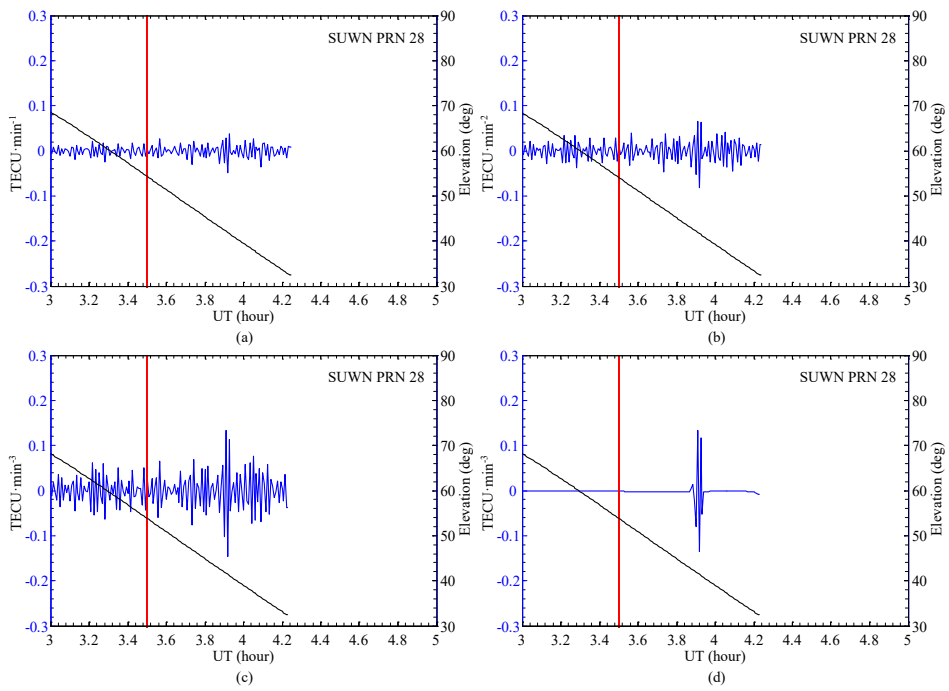


Fig. 3. Figure 3

C10

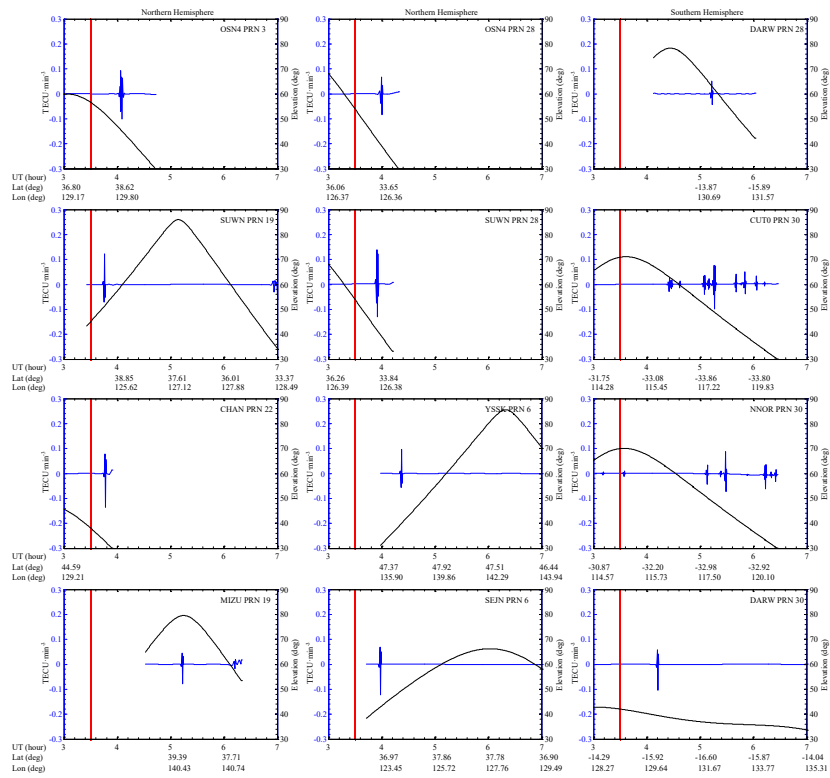


Fig. 4. Figure 4

C11

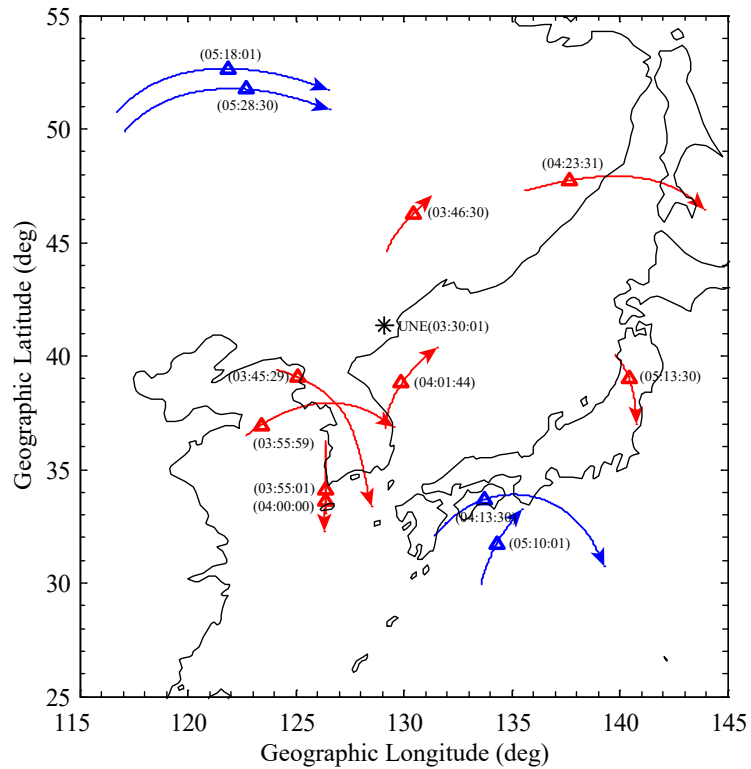


Fig. 5. Figure 5

C12

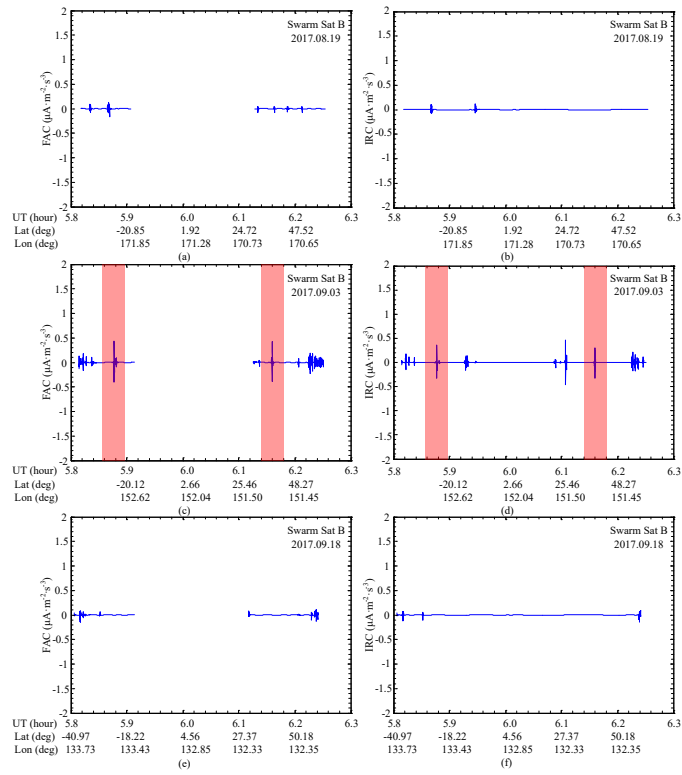


Fig. 6. Figure 6

C13

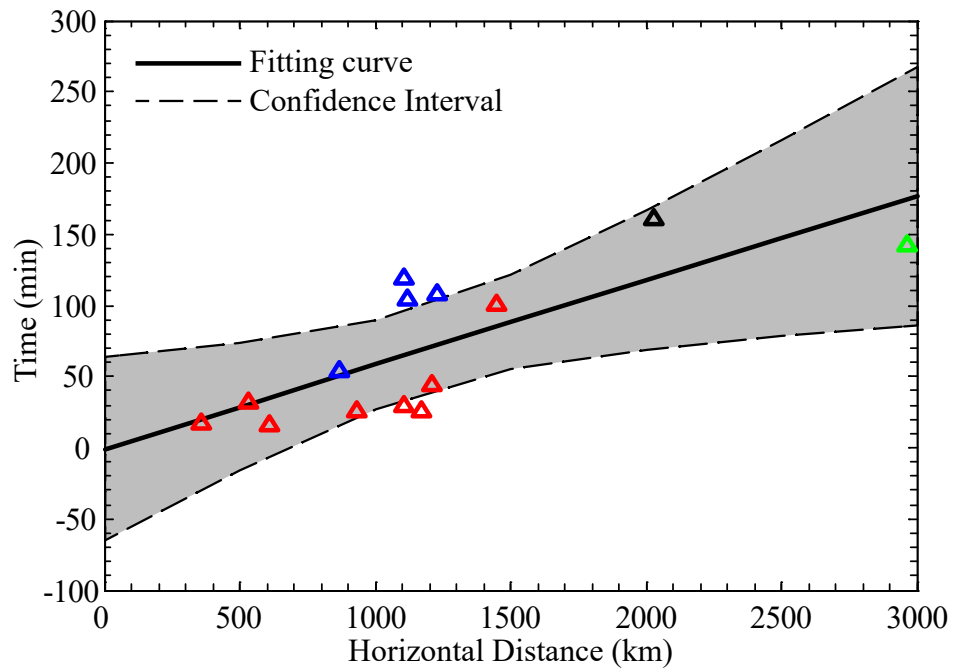


Fig. 7. Figure 7

C14

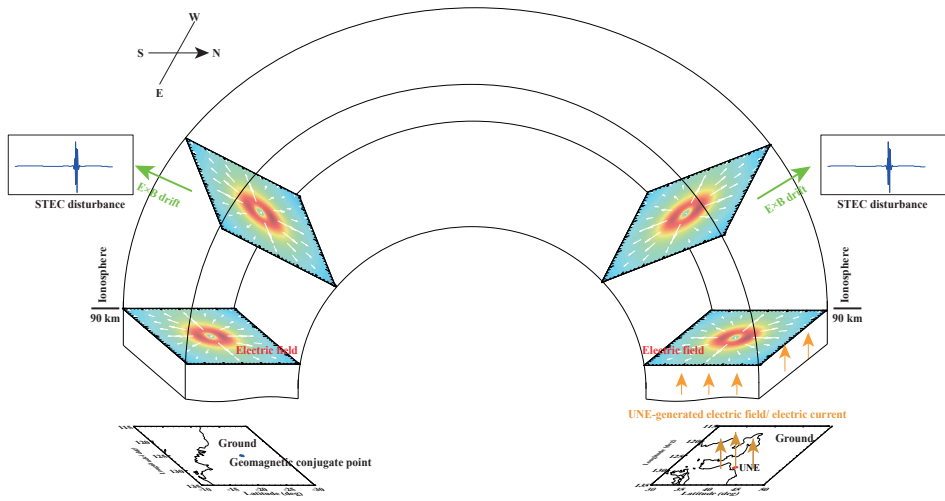


Fig. 8. Figure 8